Simulation of ozone production in a complex circulation region using nested grids

M. Taghavi, S. Cautenet, G. Foret

▶ To cite this version:

HAL Id: hal-00327865
https://hal.archives-ouvertes.fr/hal-00327865

Submitted on 25 Jul 2003

**Atmospheric
Chemistry
and Physics
Discussions**

ACPD

3, 3833–3867, 2003

Ozone simulation
using nested grids

M. Taghavi et al.

Title Page

Abstract	Introduction
Conclusions	References
Tables	Figures

◄◄	►►
◄	►
Back	Close

Full Screen / Esc

Print Version

Interactive Discussion

© EGU 2003

Simulation of ozone production in a complex circulation region using nested grids

M. Taghavi, S. Cautenet, and G. Foret

Laboratoire de Météorologie Physique, OPGC-CNRS and Université Blaise Pascal, Aubière, France

Correspondence to: M. Taghavi (M.Taghavi@opgc.univ-bpclermont.fr)

Abstract

During ESCOMPTE precampaign (15 June to 10 July 2000), three days of intensive pollution (IOP0) have been observed and simulated. The comprehensive RAMS model, version 4.3, coupled online with a chemical module including 29 species, has been used to follow the chemistry of the zone polluted over southern France. This on-line method can be used because the code is paralleled and the SGI 3800 computer is very powerful. Two runs have been performed: run1 with one grid and run2 with two nested grids. The redistribution of simulated chemical species (ozone, carbon monoxide, sulphur dioxide and nitrogen oxides) was compared to aircraft measurements and surface stations. The 2-grid run has given substantially better results than the one-grid run only because the former takes the outer pollutants into account. This online method helps to explain dynamics and to retrieve the chemical species redistribution with a good agreement.

1. Introduction

During the last century, the atmospheric composition has been considerably modified by human activities. One of the consequences of this change is the high ozone concentrations observed in polluted zones. In the recent years, strong ozone concentrations have been reported in the south of France, where there are strong anthropogenic and biogenic emissions. The ESCOMPTE campaign (2000–2001) took place in this region (Cros et al., 2003). High concentrations of ozone and other photochemical oxidants have an impact on lung functions of human beings (Bates, 1995a,b) and are recognized as having negative effects on public health, crops and forests (Taylor, 1969; Heck et al., 1984). In order to study the transport of pollutants and their chemistry regime, it is hence very important to assess the ozone production: for instance, the Current Directive 92/72/EEC for the European Union requires that the member states set and continually monitor the O_3 thresholds, with emphasis on the excess concentrations

cases (Gangoiti et al., 2002). A numerical model, describing meteorology, pollutants emission, transport, chemistry and deposition is a powerful tool to solve the problem and to allow effective control strategies. First, the model must undergo a validation step using reliable observational data, which ensures to some extent its accuracy. In fact,
5 some uncertainty is inevitable, because there are more than 3000 different chemical species in the atmosphere, involving a complex chemistry. For instance, the explicit oxidation mechanism of even one organic compound includes hundreds of reactions. Hence, the amount of reactions quickly becomes unmanageable for a VOC-NO_x mixture when the number of organics increases. An example of complex explicit mecha-
10 nism is the NCAR gas-phase master mechanism (Madronich and Calvert, 1989), with 4930 chemical reactions. Thus, there are three major problems: (i) a large CPU time is required for an explicit solution; (ii) the wide range covered by the chemical timescales leads to highly stiff systems, which requires specific solvers (Djouad and Sportisse, 2002); (iii), as a general rule, kinetic coefficients and emission rates are not available
15 for each organic species, but for a whole group. As a result, these explicit chemical mechanisms are not used in pollution studies, except to describe the inorganic NO_x chemistry, which is relatively straightforward. Condensed schemes are therefore recommended (Aumont et al., 1996). One way to reduce (condense) the problem is the lumping method. In this method, the organics with similar chemical reaction proper-
20 ties are grouped, as non-aromatic VOCs (Jenkin et al., 1997) or alkanes (Wang et al., 1998). Two approaches have been used in developing condensed mechanisms for the organic compounds. The first one groups these species according to their traditional classifications, e.g., alkanes, alkenes, and aromatics. The second one ranks the organic compounds in terms of bonding (carbon bond mechanism) (Finlayson-Pitts and
25 Jr., 2000). There are different methods to use the chemical model. It can be used as a 0 dimension or box model (Schere and Demerijan, 1978; Kuhn et al., 1998). However, Eulerian models must be used to assess realistic pollutant transport and concentrations:

- Urban-scale models: the UAM (Urban Airshed Model: Reynolds et al., 1973;

Title Page

Abstract | Introduction

Conclusions | References

Tables | Figures

◀ | ▶

◀ | ▶

Back | Close

Full Screen / Esc

Print Version

Interactive Discussion

© EGU 2003

Tesche and McNally, 1991), the CIT model (California Institute of Technology model: McRae et al., 1982b; Russell et al., 1988), and the SMOG model (Surface Meteorology and Ozone Generation model; Lu et al., 1997a,b) where the horizontal size of each grid is of the order of a few kilometers, e.g., 4 or 5 km square grids with the vertical height split into 5–20 layers of increasing thickness beginning at ground level.

– Regional-scale models: RADM (Regional Acid Deposition Model: Chang et al., 1987), ADOM (Acid Deposition and Oxidant Model: Venkatram et al., 1988), STEM II (Sulfur Transport Eulerian Model: Carmichael et al., 1991), RTM-III (Regional Transport Model III: Liu et al., 1984), LIRAQ (Livermore Regional Air Quality Model: MacCracken et al., 1978), CALGRO (Yamartino et al., 1992), and ROM (Regional Oxidant Model: Lamb, 1983), the scale is of the order of 15–130 km. The number and size of the vertical layers can vary from 6 to 30.

The chemistry models can be coupled either online or offline with the meteorological models. In offline case, care must be taken of the frequency of the sampling rate of the meteorological fields as regards transport. For example, a 3-hour frequency is used in the offline coupling of LOTOS model (VanLoon et al., 2000) whereas a 1-hour frequency is taken for TVM (meteorological model) coupled off line with the chemistry model RACM (Thunis and Cuvelier, 2000). It is evident that, in these cases, we cannot have a good accuracy of the species transport, because the meteorological data are averaged in time. The emission rates and the transport play an important role in the chemistry regime for the meso-scale studies, specially in case of complex circulation. For instance, if we use a 3-hourly meteorological dataset, a problem arises during the afternoon, as at 16 LST, may occur a sea breeze regime, whereas at 19 LST, a land breeze onset may already be effective. On the other hand, the offline method is useful in large scale studies.

The aim of this study is to find a chemistry/transport model, which reconciles two antagonistic requirements: a minimum CPU time and a maximum accuracy. To this

end, it is certainly better to use an online coupling between the meteorological and the photochemical models, since computers as SGI 3800 are very powerful and fast for paralleled codes. In this modelling, the RAMS (Regional Atmospheric Modelling Systems) meso-scale model (Cotton et al., 2003) has been coupled online with the MOCA 2.2 chemical model (Aumont et al., 1996). It is named RAMS-chemistry. We have focussed on transport, dynamical impact and chemical redistribution from primary or secondary species.

In this paper, we first remind briefly the context of ESCOMPTE precampaign. We display the emission database and the modelling. We examine the meteorological conditions during the pollution period and compare the modelled meteorological fields to the observed values (surface station and aircraft measurements). Then, we describe the chemistry mechanism (code MOCA 2.2) coupled online with RAMS. Finally, we assess the numerical results of ozone, monoxide of carbon, nitrogen oxides and sulfur dioxide in comparison with aircraft and surface observations, and we discuss their redistribution.

2. ESCOMPTE pre-campaign

The ESCOMPTE pre-campaign was conducted in June and July of 2000 in southeastern France (http://medias.obs-mip.fr/escompte/maquette/pagef.php3). During the ESCOMPTE precampaign (2000), an Intensive Observed Period (IOP0) was performed on 29, 30 June and 1 July. For these three days, we have results of meteorological and chemical surface stations and also aircraft measurements. For the modelling group, the aim of this pre-campaign was to perform runs in order to locate flight plans and surface stations. The pre-campaign includes chemical and meteorological data, which are required to run and validate the models. We have: (i) the anthropogenic and biogenic emissions with two different resolutions (15 km and 3 km); (ii) information about meteorological situation during the pollution period; (iii) surface measurement (fix and mobile stations) for both meteorological and chemical data; (iv)

Ozone simulation using nested grids

M. Taghavi et al.

Title Page

Abstract	Introduction
Conclusions	References
Tables	Figures

◄ | ►|

◄ | ►

Back | Close

Full Screen / Esc

Print Version

Interactive Discussion

Ozone simulation using nested grids

M. Taghavi et al.

© EGU 2003

airborne measurements (aircraft and balloon). Two aircrafts were operated: the PIPER AZTEC of Météo France and the ARAT ATR-42 of INSU (Institut National des Sciences de l'Univers), with several flights during the studied days. Some of the main objectives of the ESCOMPTE campaign are to answer the following questions:

5   1. What is the respective role of the various dynamic and chemical mechanisms on the pollutants redistribution ?

2. How to take the urban emissions in the regional or global models into account?

3. Can we develop an operational forecast of pollution period?

4. What strategy is necessary to develop in order to reduce the pollutants concen-
10   tration ?

3.   Meteorological modelling description

The RAMS (Regional Atmospheric modelling System; http://www.atmet.com; Cotton et al., 2003) model is a paralleled mesoscale model allowing the simulation of meteorological fields with horizontal scale spanning from one kilometer to about one hundred
15   kilometers. It includes nested grids. Many investigations on regional pollution were previously made using RAMS model (Lyons et al., 1995; Millan et al., 1997; Edy and Cautenet, 1998; Cautenet et al., 1999; Poulet et al., 2003).
Simulations have been performed using two nested grids simultaneously to take the synoptic and local circulations into account. In a simulation with 2 nested grids, each
20   grid covering a particular domain size (Fig. 1), a two-way interactive process is involved. Grid1 covered southern France, a part of the Northern Spain and a part of the northern Italy, resulting in 36 square meshes of 15km. Grid2 represents the ES-COMPTE domain. It has 52 meshes of 3 km. We used a time step of 10 s and 35 levels in the vertical dimension (the same in both grids) with 15 levels from surface to 1500 m,
25   which ensured a fine description of the boundary layer. The coarse domain included

the Lyons, Turin and Barcelona cities to the north, east and southwest respectively. Moreover, it comprised the Pyrenees, Massif Central and Alps mountains. This topography introduces a complex circulation associated with sea breeze. In the fine grid (Grid2), we have Marseilles, Toulon and Avignon cities with the Alpilles hills, the Durance and Rhone valleys. The meteorological fields have been initialized and nudged every 6 hours by ECMWF (European center for Medium-Range Weather Forecasts) database. The simulation started on 28 June 2000 at 00:00 UTC and ends on 1 July, 20:00 at 21:00 UTC. The soil vegetation model included 30 classes issued from USGS (United States Geophysical Survey) at a 1 km resolution. The patches configuration allowed us to keep the 1 km information. The topography at a 1 km resolution was also provided by USGS. The sea surface temperature was obtained from satellite and OOM (Observatoire d'Océanographie de Marseille) for the shore data.

4. Emissions

4.1. Anthropogenic emissions

A key point of the atmospheric chemistry is the influence of human activity on emissions. For example, humans have doubled the natural rate of N fixation (Vitousek et al., 1997). In fact, one of the important reasons to study atmospheric chemistry in southeastern France is the high anthropogenic emission due to many industrial factories, a great number of oil refineries, EDF (France Electricity) power stations and other large factories such as "Air Liquide" situated in the industrial zone of Fos-Sur-Mer or Berre Pond. In addition, highways and the polluted cities such as Marseilles and Toulon, in shore, and Aix-en-Provence or Avignon, inland, increase the emissions. These high anthropogenic emissions are illustrated in Fig. 2, where the NO_x emissions are shown at 12:00 UTC for an ordinary day of July.

4.2. Biogenic emission

This region is covered by a Mediterranean vegetation, providing important biogenic emission. In France, the results of experimental data indicate a periodical annual evolution of biogenic emissions characterized by a rapid growth from March up to a maximum reached in July–August, followed by a net decrease in September–October. Isoprene appears as the most abundant species (Simon et al., 2001). This compound is mainly due to Holm oak. In Fig. 3, we can see the isoprene emission at 12:00 UTC for an ordinary day of July.

4.3. Database

For Grid1 with a resolution of 15 km, the emissions were obtained from GENEMIS database. For the fine domain (Grid2), we used an inventory derived from GENEMIS and additional local data gathered in the ESCOMPTE region (http://medias.obs-mip.fr:8000/escompte). For both grids, emissions were calculated from data of 1994 for anthropogenic emission and 1997 for biogenic emission. Hourly values were used for each mesh and for two days: 5 and 6 July 1994 for anthropogenic sources and 21 and 22 July 1997 for biogenic sources. A new and more realistic inventory with a high resolution (1 km) specially dedicated to the ESCOMPTE experiment will be available in 2003.

5. Two-way nesting

In mesoscale chemical and meteorological modelling, the boundary conditions must be specified. Modelling can be strongly influenced by them, especially, when there is a strong flow crossing the borders. For chemistry/transport models, the existence of a high emission near the study domain can not be insignificant because a strong wind will transport a large amount of the emitted pollutants from the outside source inside modelling domain. The boundary conditions can be provided by global modelling

results, which generally have a resolution of about 50×50 km or more. This crude resolution is not sufficient to obtain realistic results with respect to chemistry. In our study, we want to realistically retrieve the chemical fields in Grid2. In fact, the coarse grid or Grid1 (15×15 km) was used to provide boundary values for the fine grid or Grid2

5 (3×3 km). Two-way nesting is very important to obtain realistic simulations because at each time step, the fine grid (Grid2) provides its data to the coarse (mother) grid, which in turn forces the fine (daughter) grid. The two grids communicate with each other in a two-way scheme described in Clark and Farley (1984). In particular, such a scheme allows emissions far outside Grid 2 to influence pollutant budget within this Grid2. For

10 instance, we take the emissions of pollutants from Lyons, Barcelona and Turin cities into account. The pollutants from Lyons are channeled in the Rhone valley and have an impact on the ozone production in the ESCOMPTE domain.

6. High-resolution meteorological simulation: comparison with the surface data and airborne measurements

15 The redistribution of pollutants and therefore the ozone production is very dependent on meteorological conditions. The observed meteorological situation during IOP0 is summarized in Table 1. Generally, it is not cloudy. On 29 June, the west-northwesterly wind prevailed; on 30 June, a sea breeze developed; finally, on 1 July, the sea breeze was intensified by a southwesterly flow.

20 To validate the simulated meteorological fields, we compare the model results to surface observations and airborne measurements. Some of these comparisons are shown in Figs. 4 and 5. To compare the model issues with the station data, we use the statistical method (Cai and Steyn, 2000). In fact, we have many stations: about 5 for each of the 4 towns in the model area (Marseilles, Toulon, Marignane and Avignon).

25 These data can be strongly influenced by local effects. Marseilles and Toulon are located near the shore; Marignane lies in the center of the domain; Avignon is the furthest in land. The station data referred to as "hourly" have been averaged over the

last 15 minutes. In Fig. 4, we note that the observed and modelled temperature for the three days of IOP0 are in good agreement for all surface stations, the same for the wind speed in Fig. 4.

With respect to airborne data (Figs. 5 and 6), potential temperature, specific humidity,
wind speed and direction measurements are in good agreement with modelled values. However, we note some small differences for potential temperature, wind speed and direction around 51500s and 54500s (Fig. 5). In these times AZTEC is situated in low level (Fig. 7) where the altitude is drawn versus time. For ARAT, wind speed and direction are different around 38500s (Fig. 6) in free troposphere (Fig. 7), and for wind
direction and specific humidity around 45000s (Fig. 6) in low levels (Fig. 7 for ARAT). Finally, we can say that the simulated meteorological fields are very realistic and then they cannot involve a bias for chemical fields.

7. Chemical model

The mechanism used is given in Annex 1. It is a condensed version of MOCA 2.2 (Au-
mont et al., 1996). It takes 29 species and 64 reactions into account. It can account for the main processes driving the ozone concentration in a polluted zone. The hydroper-oxyl/ aldehyde conversion allows to describe the degradation of the various organic compounds from the anthropogenic emissions. The main 3 ways of isoprene oxidation (strongly emitted by Mediterranean forest) are taken into account. Our chemical mod-
ule calculates PAN concentration, which allows to represent NO_y transport. Lastly, the model includes NO_3/N_2O_5 equilibrium for night chemistry.

The chemical solver is the QSSA or Quasi Steady State Approximation (Hesstvedt et al., 1978), faster than matrix solver like Gear solver (Gear, 1971), but quite accurate (Shieh et al., 1988; Dabdud and Seinfeld, 1995; Saylor and Ford, 1995). At each time
step and each mesh, chemical rates are evaluated from temperature and pressure calculated in the RAMS model. Photolysis rates are estimated from Madronich model (Madronich, 1987), which takes solar incident radiation and molecular properties of

atmospheric gases into account. These rates are updated every five minutes. Actinic fluxes are estimated by delta-Eddington approximation (Joseph et al., 1976; Wiscombe, 1997). Three photolysis reactions, not integrated in the Madronich's program, have been added in this model: the quantum yield and the absorption efficiency (Aumont
5 et al., 1996).

To reduce the CPU time calculation, we have developed an original way of chemical constant rate evaluation (Poulet et al., 2003). Chemical kinetic coefficients are calculated from a complex expression dependent on temperature and pressure. Since temperature and pressure vary at every mesh, calculations are made for each of them
10 and therefore require a very long time. In our scheme, a lookup table has been created for each chemical kinetic coefficient before simulation for all the temperature and pressure conditions in the atmosphere. So, during the run, RAMS-chemistry merely chooses the coefficient fitted to the meteorological conditions in the lookup table. The interest of such a method with a paralleled code is that CPU time is short: it allows to
15 strongly reduce the simulation time (for SGI 3800 computer : 1h30 CPU for a simulated day).

8. Chemical results

In the ESCOMPTE region, the emissions are mainly anthropogenic and are located along shore (Fig. 2), and specially around the Berre Pond, but there are also bio-
20 genic emissions from the forest inland (Fig. 3). In the troposphere, ozone production is dependent on many parameters such as: dynamical conditions, radiation intensity, NO_x/VOC ratio, etc.. It is sensitive to VOC and NO_x emissions (Weimin et al., 1997). The maximum in ozone occurs when there is a high concentration in VOC and NO_x that can be due to emission or transport (Dodge, 1997b; Finlayson-Pitts and Jr., 1993).
25 The sensitivity of ozone production to each of these parameters is variable. If one of these parameters is not taken into account correctly, an error in ozone concentration occurs.

Ozone simulation using nested grids

M. Taghavi et al.

Title Page

Abstract	Introduction
Conclusions	References
Tables	Figures

◄◄	►►
◄	►
Back	Close

Full Screen / Esc

Print Version

Interactive Discussion

Two runs are performed: run1 with one grid, Grid 2 which represents the ES-COMPTE region; run2 with two nested grids (Grid1 and Grid2). To evaluate the skill of RAMS-chemistry model, we compare the aircraft and surface stations measurements with numerical results. During the run, at each time step, the coordinates of aircraft (altitude, latitude, longitude) are noted and the fitted numerical values are written in a file. Then the modelled values correspond exactly to the same place and the same time than aircraft.

8.1. Aircraft measurements

Figure 7 presents the comparisons between model results and airborne data during IOP0 for run1 and run2. For both flights (AZTEC and ARAT), the modelled ozone curve follows the observed ozone curve (same maximum and minimum), with, however, a weak, but systematic underestimation in model values. We think this difference could originate from two reasons: (i) our chemical model includes the main species, but not all, and (ii) errors can exist in emissions rates data and in sources locations. Recall that these emissions were calculated from a 1994 database for anthropogenic emissions and from a 1997 file for biogenic emissions. When the aircraft altitude is high, i.e. when the measurements are performed within the free troposphere, we note weak ozone values. For the lower levels, near the ground, the values are generally high, except for the landing. Planes took off and landed at Marignane airport, which is very close to high emissions sources of NO_x and they flied at low altitudes over smokestacks. In this case, where there are a high NO_x concentrations, the ozone titration is very probable, especially in the absence of sufficient amount of VOC, or in other term, when the NO_x/VOC ratio is not favorable (Finlayson-Pitts and Jr., 2000). However, we remark that for both flights, run2 which takes the pollution from Grid1 into account gives better results than run1.

© EGU 2003

8.2. Surface stations

For some surface stations, the numerical results are compared with the ozone, carbon monoxide, sulphur dioxide and nitrogen oxide observations. Figure 8 shows that for four stations, the ozone results of run2 follow better the observations than run1. In
Avignon, town located to the north of Grid2 (Fig. 1), on 29 and 30 June (01:00 UTC to 48:00 UTC), the ozone values are higher than on 1 July (48:00 UTC to 72:00 UTC) (Fig. 8). On 29 June, the values are above 70 ppb because of transport of pollutants from northern areas. On the contrary, in Marignane, Toulon and Marseilles, towns located near shore (Fig. 1), the maxima of ozone are found for 30 June. During this
day, the wind is weak and the sea breeze is well developed, we have a maximum of 80 ppb at Toulon and 70 ppb at Marignane. In Fig. 9, for two stations (Marseilles and Aix), the NO_x measurements are slightly different from numerical results for both runs. Again, we note that run2 is always better than run1. The observations show that the NO_x are limited only at Aix on 29 June. The same occurs at Aix and Marseilles on
1 July (which is a Saturday). The NO_x levels are very strong for both towns on 30 June which is a Friday (a day of departure for summer holidays). In Fig. 9, we can see the CO variations for the three days. The levels are high, particularly on 30 June and 1 July. The numerical results are better the first day (where the traffic is regular) than the next days. In Fig. 9 we display the time evolution of the SO_2 concentration for two
stations (Aix and Avignon). In Aix, there is a local SO_2 emission. In Avignon, the levels are low, except on the last day because of synoptic transport (Southerly flow). For both cases, run2 is slightly better than run1.

We have examined four compounds during three days, and each of them has a different time evolution due to their differences in nature: ozone is a secondary pollutant;
CO is an inert tracer; NO_x is a primary pollutant and is driven by photochemistry; finally, SO_2 is a primary pollutant.

8.3. Discussion

For the four stations of Marignane, Marseilles, Toulon and Avignon, and during the three days of IOP0, we have an ozone peak every day, in spite of the fact that the meteorological and chemistry regimes are very different. The first day (Thursday, 29 June) is a normal day as regards emissions, because the levels of CO, SO_2 and NOx concentrations are not very high (Fig. 9, from 00:00 to 24:00 UTC). The sea breeze is weak and is associated with a northerly synoptic flow (Mistral). The ozone production is more important in Avignon than in the other cities because the channelling along the Rhone valley brings the pollutants from the north region. In this case, the impact of Lyons city must be taken into account and this is the reason, for which run2 is better than run1. For this day, in Fig. 10, we can see that the maximum in ozone at 09:00 UTC in Grid 2 is due to the northerly flow which transports the pollutants along the Rhone valley.

The second day (30 June), the traffic is very important because it is the departure of summer holidays, so that the emissions are wrong because they refer to a normal day. We can see in Fig. 9, from 24:00 to 48:00 UTC, that the high levels of NO_x and CO are not retrieved by either run1 or run2. On the contrary, the SO_2 concentration is well retrieved. We are in the case where the inventory is not adapted for NO_x and CO. During this day, the northerly wind is weak and the sea breeze is well developed. Photochemistry is active and ozone peaks are higher near the shore (Marignane, Marseilles and Toulon) than inland (Avignon).

On the third day (1 July), we can see in Fig. 9, from 48:00 to 72:00 UTC, that the CO concentration is still high because it is an inert gas, and, moreover, the wind is weak and therefore the diffusion is not efficient. During this day (Saturday), the traffic is less important than during the previous day. The sea breeze is associated with a weak southwesterly wind. The photochemistry is active and we have an ozone production with limited NO_x (Dodge, 1997b; Finlayson-Pitts and Jr., 1993). We remark that SO_2 concentration is higher in Avignon than during the previous days at this same place,

where there is no emission, because of the southwesterly flow.

Although the 30 June and the 1 July present different chemistry and meteorological conditions, the ozone values are fairly retrieved in both the mixed boundary layer and the free troposphere (Fig. 7).

Throughout this study, the numerical results from run2 explain better the redistribution of chemical species than those from run1. However, this method is more relevant to retrieve the ozone concentration, which is a secondary species than the concentration of primary compounds like NO_x or SO_2 in a polluted region. We have remarked that the emission inventory has a strong impact for the species locally emitted. Further investigation using the measurements of the campaign in 2001, will compare the results obtained from this inventory and a new one specially built for the ESCOMPTE experiment.

9. Conclusions

RAMS-Chemistry, the RAMS code coupled online with a chemistry model (MOCA 2.2), including 29 species, allows to retrieve the main maxima of ozone and to follow the photochemistry of a polluted zone. In the view of saving CPU time, the chemical kinetic coefficients and photolysis rates are precalculated into look up tables. The CPU time is 1H30 on SGI 3800 computer for a simulated day over the ESCOMPTE domain. Two runs are performed. Run1 with one grid and run2 with two nested grids. The simulated meteorological fields (wind, temperature, humidity) and ozone redistribution are compared with aircraft measurements and four surface stations during IOP0. Primary species like carbon monoxide, nitrogen oxides and sulfur dioxide are investigated in several stations. The 2-grid run looks substantially better than the one grid run because the former takes the outer pollutants into account. However, this method is more relevant to retrieve the ozone concentration, a secondary species, than the concentration of primary compounds like NO_x or SO_2 which are closely linked to emission sources. The impact of the channeling along the Rhone valley has been demonstrated

with run2. Dynamical processes (synoptic flow and the sea-breeze circulation) are involved to explain the ozone production and the redistribution of CO, NO_x and SO_2.

We can conclude that the condensed chemistry code satisfactorily simulates the chemical species redistribution for an urban polluted zone where the meteorological circulations are complex (topography and sea breeze).

References

Aumont, B., Jaecker-Voirol, A., Martin, B., and Toupance, G.: Tests of some Reduction Hypotheses Made in Photochemical Mechanisms, Atmos. Envir., 30, 2061–2077, 1996. 3835, 3837, 3842, 3843

Bates, D. V.: Ozone: A Critical Review of Recent Experimental, Clinical and Epidemiological Evidence, with Notes Causation, Part1, Can. Resp. J., 2, 25–31, 1995a. 3834

Bates, D. V.: Ozone: A Critical Review of Recent Experimental, Clinical and Epidemiological Evidence, with Notes Causation, Part2, Can. Resp. J., 2, 161–171, 1995b. 3834

Cai, X.-M. and Steyn, D.: Modelling Study of Sea Breezes in a Complex Coastal Environment, Atmos. Envir., 34, 2873–2885, 2000. 3841

Carmichael, G. R., Peters, L. K., and Saylor, R. D.: The STEM-II Regional Scale Acid Deposition and Photochemical Oxidant Model. I. An Overview of Model Development and Applications, Atmos. Envir., 25, 2077–2090, 1991. 3836

Cautenet, S., Poulet, D., Delon, C., Delmas, R., Grégoire, J., Pereira, J., Cherchali, S., Amram, O., and Flouzat, G.: Simulation of Carbon Monoxide Redistribution over Central Africa During

Ozone simulation using nested grids

M. Taghavi et al.

Title Page

Abstract	Introduction
Conclusions	References
Tables	Figures

◄ | ►

◄ | ►

Back | Close

Full Screen / Esc

Print Version

Interactive Discussion

© EGU 2003

Biomass Burning (Experiment for Regional Sources and Sinks of Oxidants, EXPRESSO), J. Geophys. Res., 104, 30 641–30 657, 1999. 3838

Chang, J. S., Brost, R. A., Isaksen, I. S. A., Madronich, S., Middleton, P., Stockwell, W. R., and Walcek, C. J.: A Three-Dimensional Eulerian Acid Deposition Model: Physical Concepts and Formulations, J. Geophys. Res., 92, 14 681–14 700, 1987. 3836

Clark and Farley: Severe Downslope Windstorm Calculations in Two and Three Spatial Dimensions Using Anelastic Interactive Grid Nesting: A Possible Mechanism for Gustiness, Journal of the Atmospheric Sciences, 41, 329–350, 1984. 3841

Cotton, W., Sr, R. P., Walko, R. L., Liston, G. E., Tremback, C., Jiang, H., McAnely, R., Harrington, J., Nicholls, M., Carrio, G., and McFadden, J.: Rams 2001: Current Status and Future Directions, Meteorol. Atmos. Phys., 82, 5–29, 2003. 3837, 3838

Cros, B., Durand, P., and Ponche, J. L.: The ESCOMPTE Program: An Overview, Atmos. Res., 2003. 3834

Dabdud, D. and Seinfeld, J. H.: Extrapolation Techniques Used in the Solution of Stiff Odes Associated with Chemical Kinetics of Air Quality Models, Atmos. Envir., 29, 403, 1995. 3842

Djouad, R. and Sportisse, B.: Solving Reduced Chemical Models in Air Pollution Modeling, Appl. Numer. Math., 2002. 3835

Dodge, M. C.: Combined Use of Modelling Techniques and Smog Chamber Data to Derive Ozone-Precursor Relationships, in Proceedings of the International Conference on Photochemical Oxidant Pollution and its Control, EPA-60/3-77-001b, edited by Dimitriades, B., 2, 881–889, 1997b. 3843, 3846

Edy, J. and Cautenet, S.: Biomass Burning : Local and Regional Redistribution, Air Pollution Modeling and its application, pp. 63–69, 1998. 3838

Finlayson-Pitts, B. J. and Jr., J. N. P.: Volatile Organic Compounds: Ozone Formulation, Alternative Fuels, and Toxics, Chem. Ind., October 18, 796–800, 1993. 3843, 3846

Finlayson-Pitts, B. J. and Jr., J. N. P.: Chemistry of the Upper and Lower Atmosphere, Academic Press, 2000. 3835, 3844

Gangoiti, G., Alonsoa, L., Navazoa, M., Albizurib, A., Perez-Landac, G., Matabuenaa, M., Valdenebroa, V., Maruria, M., Garcia, J., and Millan, M. M.: Regional Transport of Pollutants over the Bayof Biscay: Analysis of an Ozone Episode under a Blocking Anticyclone in West-Central Europe, Atmos. Envir., 36, 1349–136, 2002. 3835

Gear, C.: Numerical Initial Value Problems in Ordinary Differential Equations, Prentice-Hall, Englewood Cliffs, New Jersey, 1971. 3842

Ozone simulation using nested grids

M. Taghavi et al.

Title Page

Abstract	Introduction
Conclusions	References
Tables	Figures

◄◄   ►►

◄   ►

Back   Close

Full Screen / Esc

Print Version

Interactive Discussion

Heck, W. W., Cure, W. W., Rawlings, J. O., Zaragoza, L. J., Heagle, A. S., Heggestead, H. E., Kohut, R. J., Kress, L. W., and Temple, P.: Assessing Impacts of Ozone on Agricultural Crops, II, Crop Yield Functions and Alternative Exposure Statistics, J. Air Pollut. Control Ass., 34, 810–817, 1984. 3834

Hesstvedt, E., Hov, O., and Isaksen, I. S.: Quasy Steady State Approximations in Air Pollution Modeling : Comparison of Two Numerical Schemes for Oxidant Prediction, Int. J. Chem. Kin., 10, 971, 1978. 3842

Jenkin, M. E., Saunders, S. M., and Pilling, M. J.: The Tropospheric Degradation of Volatile Organic Compounds: A Protocol for Mechanism Development, Atmos. Envir., 31, 81–104, 1997. 3835

Joseph, J. H., Wiscombe, W. J., and Weinman, J. A.: The Delta-Eddington Approximation for Radiative Flux Transfer, J. Atmos. Sci., 33, 2452–2459, 1976. 3843

Kuhn, M., Builtjes, P. J. H., Poppe, D., Simpson, D., Stockwell, W. R., Andersson-Sköld, Y., Baart, A., Das, M., Hov, F. F., Kirchner, F., Makar, P. A., Milford, J. B., Roemer, M. G. M., Ruhnke, R., Strand, A., Vogel, B., and Vogel, H.: Intercomparaison of the Gase-Phase Chemistry in Several Chemistry and Transport Models, Atmos. Envir., 32, 693–709, 1998. 3835

Lamb, R. G.: Regional Scale (1000 km) Model of Photochemical Air Pollution, Part 1. Theoretical Formulation, Tech. rep., Environmental Sciences Research Laboratories, Research Triangle Park, North Carolina, ePA/600/3-83-035, 1983. 3836

Liu, M. K., Morris, R. E., and Killus, J. P.: Development of a Regional Oxidant Model and Application to the Northeastern United States, Atmos. Envir., 18, 1145–1161, 1984. 3836

Lu, R., Turco, R. P., and Jacobson, M. Z.: An Integral Air Pollution Modeling System for Urban and Regional Scales: 1. Structure and Performance, J. Geophys. Res., 102, 6063–6079, 1997a. 3836

Lu, R., Turco, R. P., and Jacobson, M. Z.: An Integral Air Pollution Modeling System for Urban and Regional Scales: 2. Simulation for SCAQS, J. Geophys. Res., 102, 6081–6098, 1997b. 3836

Lyons, A., Tremback, C. J., and Pielke, R. A.: Applications of the Regional Atmospheric Systems (RAMS) to Provide Input to Photochemical Grid Models for the Lake Michigan Ozone Study (LMOS), J. Appl. Meteor, 34, 1762–1785, 1995. 3838

MacCracken, M. C., Wuebbles, D. J., Walton, J. J., Duewer, W. H., and Grant, K. E.: The Livermore Reginal Air Quality Model. I. Concept and Development, J. Appl. Meteorol., 17,

254–272, 1978. 3836

Madronich, S.: Photodissociation in the Atmosphere. 1. Actinic Flux and the Effects of Ground Reflections and Clouds, J. Geophys. Res., 92, 9740, 1987. 3842

Madronich, S. and Calvert, J. G.: The NCAR Master Mechanism of the Gas Phase Chemistry, Technical Note 2.0, NCAR, 1989. 3835

McRae, G. J., Goodin, W. R., and Seinfeld, J. H.: Development of Second-Generation Mathematical Model for Urban Air Pollution -I. Model Formulation, Atmos. Envir., 16, 679–696, 1982b. 3836

Millan, M., Salvador, R., Mantilla, E., and Kallos, G.: Photooxidant Dynamics in Th Mediterranean Basin in Summer : Results from European Research Projects, J. Geophys. Res., 102, 8811–8823, 1997. 3838

Poulet, D., Cautenet, S., and Aumont, B.: Simulation of the Chemical Impact of the Bush Fires Emissions, in Central Africa, During the EXPRESSO Campaign, Submitted to J. Geophys. Res., 2003. 3838, 3843

Reynolds, S. D., Roth, P. M., and Seinfeld, J. H.: Mathematical Model of Photochemical Air Pollution, I. Formulation of the Model, Atmos. Envir., 7, 1033–1061, 1973. 3835

Russell, A. G., McCue, K. F., and Cass, G. R.: Mathematical Modeling of the Formation of Nitrogen-Containing Air Pollutants. 1. Evaluation of an Eulerian Photochemical Model, Environ. Sci. Technol., 22, 263–271, 1988. 3836

Saylor, R. D. and Ford, G. D.: On the Comparison of Numerical Methods for the Integration of Kinetic Equations in Atmospheric Chemistry and Transport Model, Atmos. Envir., 29, 2585, 1995. 3842

Schere, K. L. and Demerijan, K. L.: A Photochemical Box Model for Urban Air Quality, in Proceedings of the 4th Joint Conference on Sensing of Environmental Pollutants, pp. 427–433, Am. Chem. Soc., Washington, DC, 1978. 3835

Shieh, D. S.-S., Chang, Y., and Carmichael, G. R.: The Evaluation of Numerical Techniques for Solution of Stiff Ordinary Differential Equations Arising from Chemical Kinetic Problems, Env. Software, 3, 28–38, 1988. 3842

Simon, V., Luchetta, L., and Torres, L.: Estimating the Emission of Volatile Organic Compounds (VOC) from the French Forest Ecosystem, Atmos. Envir., 35 Supplement No. 1, S115–S126,, 2001. 3840

Taylor, O. C.: Importance of Peroxyacetyl Nitrate (PAN) as a Phototoxic Air Pollutant, J. Air Pollut. Control Ass., 19, 347–351, 1969. 3834

Ozone simulation using nested grids

M. Taghavi et al.

Title Page

Abstract	Introduction
Conclusions	References
Tables	Figures

◀◀   ▶▶

◀   ▶

Back   Close

Full Screen / Esc

Print Version

Interactive Discussion

Tesche, T. W. and McNally, D.: Photochemical Modeling of Two 1984 SCCCAMP Ozone Episodes, J. Appl. Meteorol., 30, 745–763, 1991. 3836

Thunis, P. and Cuvelier, C.: Impact of Biogenic Emissions on Ozone Formation in the Mediterranean Area – a BEMA Modelling Study, Atmos. Envir., 34, 467–481, 2000. 3836

5 VanLoon, M., Builtjes, P. J. H., and Segers, A. J.: Data Assimilation of Ozone in the Atmospheric Transport Chemistry Model LOTOS, Environmental Modelling, 15, 44, 2000. 3836

Venkatram, A., Karamchandani, P. K., and Mistra, P. K.: Testing a Comprehensive Acid Deposition Model, Atmos. Environ., 22, 737–747, 1988. 3836

Vitousek, P. M., Aber, J. D., Howarth, R, W. L., Matson, G. E., Schindler, P. A., Schlesinger,
10 D. W., and G., W. H. T. D.: Human Alteration of the Global Nitrogen Cycle : Sources and Consequences, Ecological Application, 7, 737–750, 1997. 3839

Wang, S. W., Georgopoulos, P. G., Li, G., and Rabitz, H.: Condensing Complex Atmospheric Chemistry Mechanisms. 1. The Direct Constrained Approximate Lumping (DCAL) Method Applied to Alkane Photochemistry, Environ. Sci. Technol., 32, 2018–2024, 1998. 3835

15 Weimin, J., Donald, L., Singleton, M. H., and McLaren, R.: Sensitivity of Ozone Concentrations to VOC and NO_x Emissions in the Canadian Lower Fraser Valley, Atmos. Envir., 31, 627–638,, 1997. 3843

Wiscombe, W. J.: The Delta-M Method : Rapid Yet Accurate Radiative Flux Calculations for Strongly Asymetric Phase Functions, J. Atmos. Sci., 34, 1408, 1997. 3843

20 Yamartino, R. J., Scire, J. S., Carmichael, G. R., and Change, Y. S.: The CalGrid Mesoscale Photochemical Grid Model. I. Model Formulation, Atmos. Envir., 26A, 1493–1512, 1992. 3836

Ozone simulation using nested grids

M. Taghavi et al.

Table 1. Meteorological situation during IOP0

DATE	SITUATION IN THE UPPER AIR	SITUATION AT SURFACE	CLOUDY COVERAGE	TEMPERATURE		WIND
				minimum	maximum	
June 29, 2000	Strong westerly or northwesterly flow	Regime of prevailing northwesterly flow	Partly cloudy	between 18°C and 20°C	between 29°C and 31°C	Mistral, moderate to strong, exceeding 12 m/s locally
June 30, 2000	Persistence of west-northwesterly flow	shallow low	Clear to partly cloudy	between 14°C and 19°C	around 30°C	In the early hours, the wind is directed to the northwest sector, weak to moderate (6 m/s in Arles, 4 m/s in Marignane, 5 m/s in Istres), then it turns to the west sector strengthening to 5 - 7 m/s. After 18:00 UTC it weakens, its orientation oscillates between the southwest and the southeast
July 01, 2000	Progressive gap of the ridge of height eastward, forming (training) of a minimum on the near Atlantic ocean generating a southwesterly flow	Little active front over the western country	Very cloudy the morning clearing up early in the afternoon	between 16°C and 20°C	between 25°C and 30°C	Regime of breezes. In the morning, the wind is weak (<4 m/s) In Marignane the breeze begins at about 08:00 UTC from the southwest-south and blowing at a speed of 5 to 8 m/s at 19:00 UTC. Elsewhere (Arles, Sainte Marie, Marseilles) it turns to the southeast south direction.

Table 2. Chemical mechanism (MOCA 2.2)

Chemical mechanism (MOCA 2.2)				
N°	Reaction	A	N	E
1	$O_3 + NO => NO_2$	1.8 E-12	0	1370
2	$O_3 + NO_2 => NO_3$	1.2 E-13	0	2450
3	$O_3 + OH => HO_2$	1.9 E-12	0	1000
4	$O_3 + HO_2 => OH$	1.4 E-14	0	600
5	$NO + NO_3 => NO_2 + NO_2$	1.8 E-11	0	-110
6	$NO + HO_2 => nothing$	3.7 E-12	0	-240
7	$NO_2 + NO_3 => NO + NO_2$	7.2 E-14	0	1414
8	$OH + HO_2 => nothing$	4.8 E-11	0	-250
9	$OH + H_2O_2 => HO_2$	2.9 E-12	0	160
10	$HO_2 + HO_2 => H_2O_2$	2.2 E-13	0	-620
11	$HO_2 + HO_2 + M => H_2O_2 + M$	1.9 E-33	0	-980
12	$NO_3 + HO_2 => HNO_3$	9.2 E-13	0	0
13	$NO_3 + HO_2 => OH + NO_2$	3.6 E-12	0	0
14	$NO + NO + M => NO_2 + NO_2 + M$	6.93E-40	0	-530
15	$OH + HNO_4 => NO_2$	1.5 E-12	0	-360
16	$OH + CO => HO_2$	1.5 E-13	0	0
17	$OH + CO + M => HO_2 + M$	3.66E-33	0	0

Ozone simulation using nested grids

M. Taghavi et al.

Table 2. Continued

18	NO + OH (+ M) =>HONO (+ M)	Falloff
19	NO_2 + OH (+ M) =>HNO_3 (+ M)	Falloff
20	NO_2 + HO_2 (+ M) =>HNO_4 (+ M)	Falloff
21	HNO_4 (+ M) =>NO_2 + HO_2 (+ M)	Falloff
22	NO_2 + NO_3 (+ M) =>N_2O_5 (+ M)	Falloff
23	N_2O_5 (+ M) =>NO_2 + NO_3 (+ M)	Falloff
24	OH + SO_2 (+ M) =>HO_2 + H_2SO_4(+ M)	Falloff
25	HO_2+ HO_2 =>H_2O_2	Special
26	N_2O_5 =>2HNO_3	Special
27	O_3 + hν =>2OH	Photolyse
28	O_3OLSB =>nothing	Special
29	NO_2 + hν =>NO + O_3	Photolyse
30	H_2O_2 + hν =>OH + OH	Photolyse
31	NO_3 + hν =>NO	Photolyse
32	NO_3 + hν =>NO_2 + O_3	Photolyse
33	HONO + hν =>NO + OH	Photolyse

[Print Version](#)

[Interactive Discussion](#)

Ozone simulation using nested grids

M. Taghavi et al.

© EGU 2003

Table 2. Continued

34	$<RO_2> + NO => NO_2 + HO_2$	4. 2E-12	0	-180
35	$<RO_2> + HO_2 => ROOH$	4. 1E-13	0	-790
36	$<NONO_2> + NO => NO_2$	4. 2E-12	0	-180
37	$<NONO_2> + HO_2 => ROOH$	4. 1E-13	0	-790
38	$OH + HCHO => HO_2 + CO$	1.25E-17	2	-648
39	$OH + CH_3CHO => CH3COO_2$	5.55E-12	0	-311
40	$CH_3COO_2 + NO => NO_2 + HCHO + <RO_2>$	2.0E-11	0	0
41	$HO_2 + CH3COO_2 => 0.3\ O_3 + 0.7\ ROOOH$	4.3E-13	0	-1040
42	$C_2H_5CHO + OH => C_2H_5COO_2$	8.5E-12	0	-252
43	$C_2H_5COO_2 + NO => NO_2 + CH_3CHO + <RO_2>$	2.0E-11	0	0

Table 2. Continued

44	$C_2H_5COO_2$ + HO_2 =>0.3 O_3 + 0.7 ROOOH	4.3E-13	0	-1040
45	$C_2H_5COO_2$ + NO_2 =>PPN	8.4E-12	0	0
46	PPN =>$C_2H_5COO_2$ + NO_2	1.6E17	0	14073
47	O_3OLSB + SO_2 =>H_2SO_4	1.0E-13	0	0
48	ROOH + OH =>OH	1.0E-12	0	-190
49	ROOH + OH =><RO_2>	1.9E-12	0	-190
50	ROOH + OH =><RO_2>	Falloff		
51	CH_3COO_2 + NO_2 (+M) =>PAN (+M)	Falloff		
52	PAN (+M) =>CH_3COO_2 + NO_2 (+M)	Photolyse		
53	HCHO + $h\nu$ =>2HO_2 + CO	Photolyse		
54	HCHO + $h\upsilon$ =>CO	Photolyse		
55	CH_3CHO + $h\nu$ =>HCHO + <RO_2>+HO_2 + CO	Photolyse		
56	C_2H_5CHO + $h\nu$ =>CH_3CHO + <RO_2>+HO_2 + CO	Photolyse		
57	C_3H_6 + OH =>CH_3CHO + HCHO + <RO_2>	4.85E-12	0	-504
58	C_3H_6 + OH =>CH_3CHO + HCHO + <RO_2>	2.54E-11	0	-410
59	ISOP + O_3 =>0.5 HCHO + 0.5 C_2H_5CHO+ 0.275 O_3OLSB + 0.4 CO + 0.28 HO_2+ 0.34 CH_3CHO + 0.07 C_2H_6 + 0.15 OH + 0.31 <RO_2>	1.23E-14	0	2013
60	ISOP + NO_3 =>HCHO + C_2H_5CHO + NO_2+ <$NONO_2$>	2.54E-11	0	1080
61	O_3 + C_3H_6 =>0.53 HCHO + 0.5 CH_3CHO + 0.225 O_3OLSB + 0.28 HO_2 + 0.4 CO + 0.31 HCHO + 0.31 <RO_2>+ 0.07 CH_4+ 0.15 OH	5.51E-15	0	1878
62	C_2H_6 + OH =>CH_3CHO + <RO_2>	4.85E-12	0	-504
63	C_2H_4 + $O3$ =>HCHO + 0.37 O_3OLSB+ 0.44 CO + 0.12 HO_2	9.14E-15	0	2580
64	C_2H_4 + OH =>a1 HCHO + a2 CH_3CHO + <RO_2>	1.96E-12	0	-438
where the stoechiometric coefficients a1 and a2 depend on temperature				

Ozone simulation using nested grids

M. Taghavi et al.
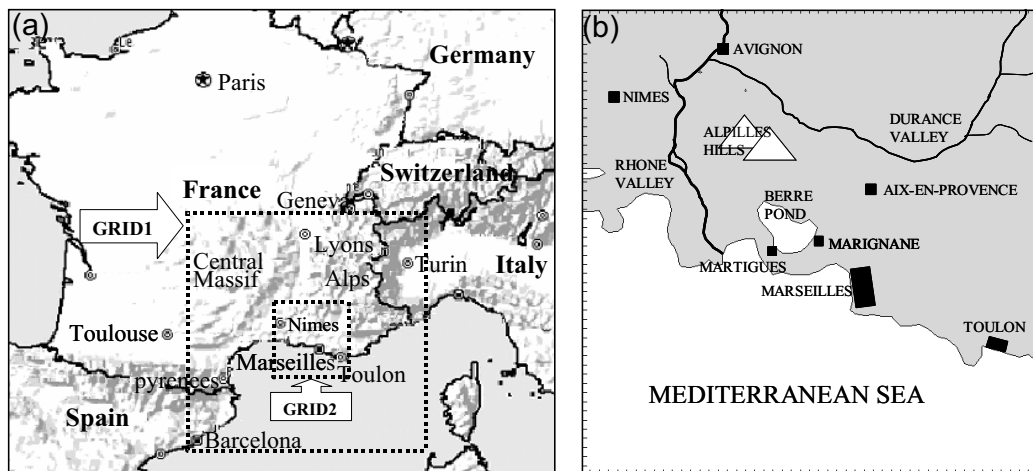
Fig. 1. **(a)** Geographical map and configuration of nested grids, grid 2 represents the ES-COMPTE domain; **(b)** A zoom on grid 2 with location of some observation stations.
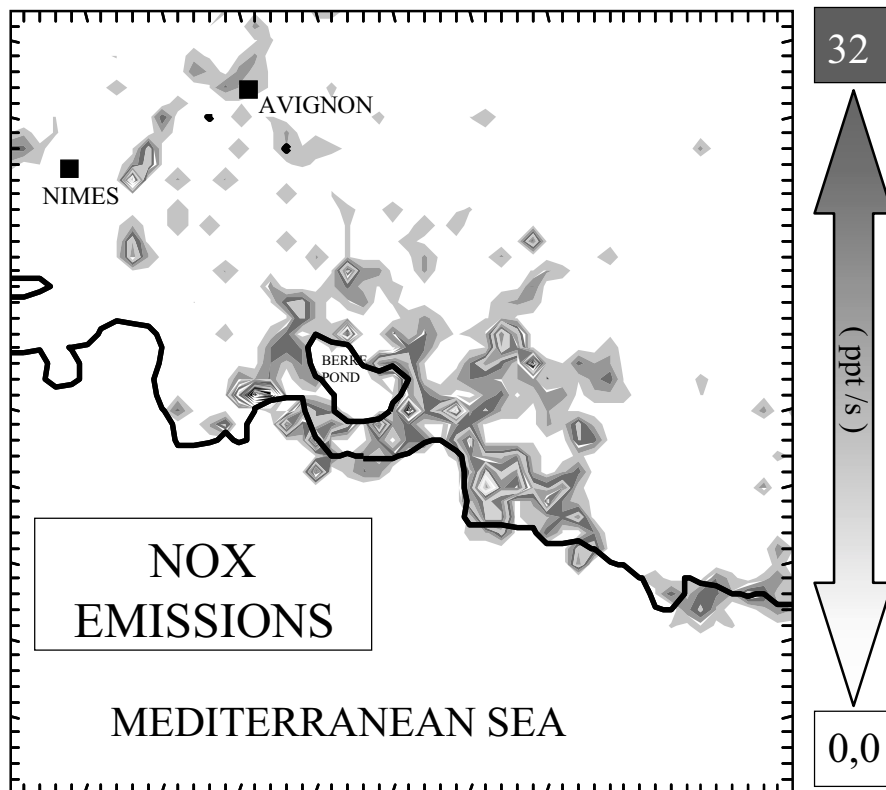
Fig. 2. NO_x emission map for an ordinary day of July at 12:00 UTC.
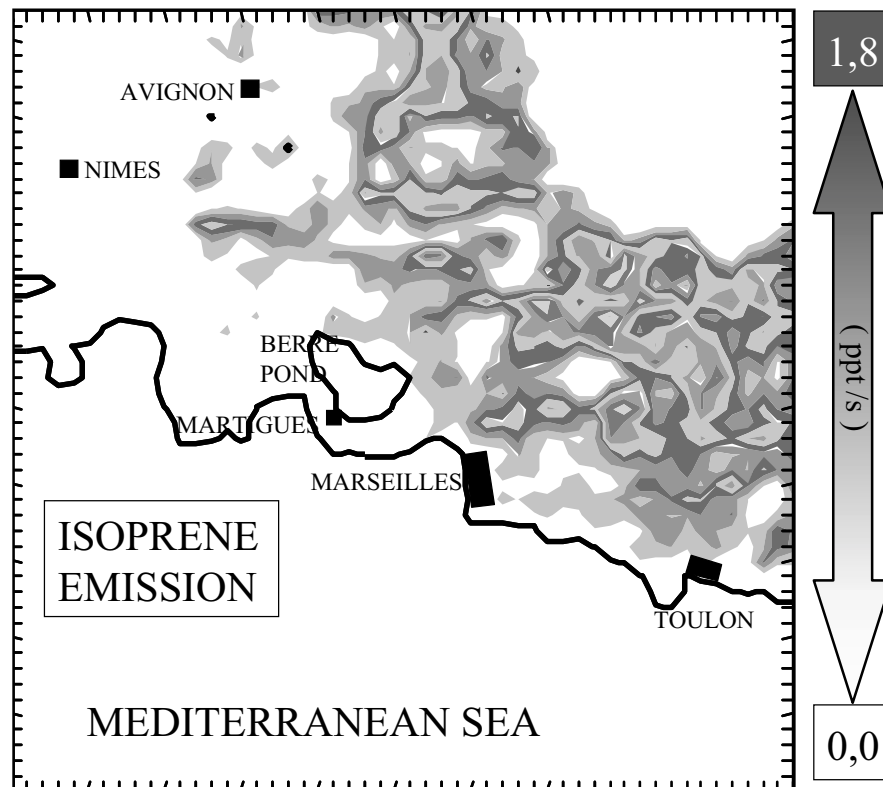
Fig. 3. Isoprene emission map for an ordinary day of July at 12:00 UTC.
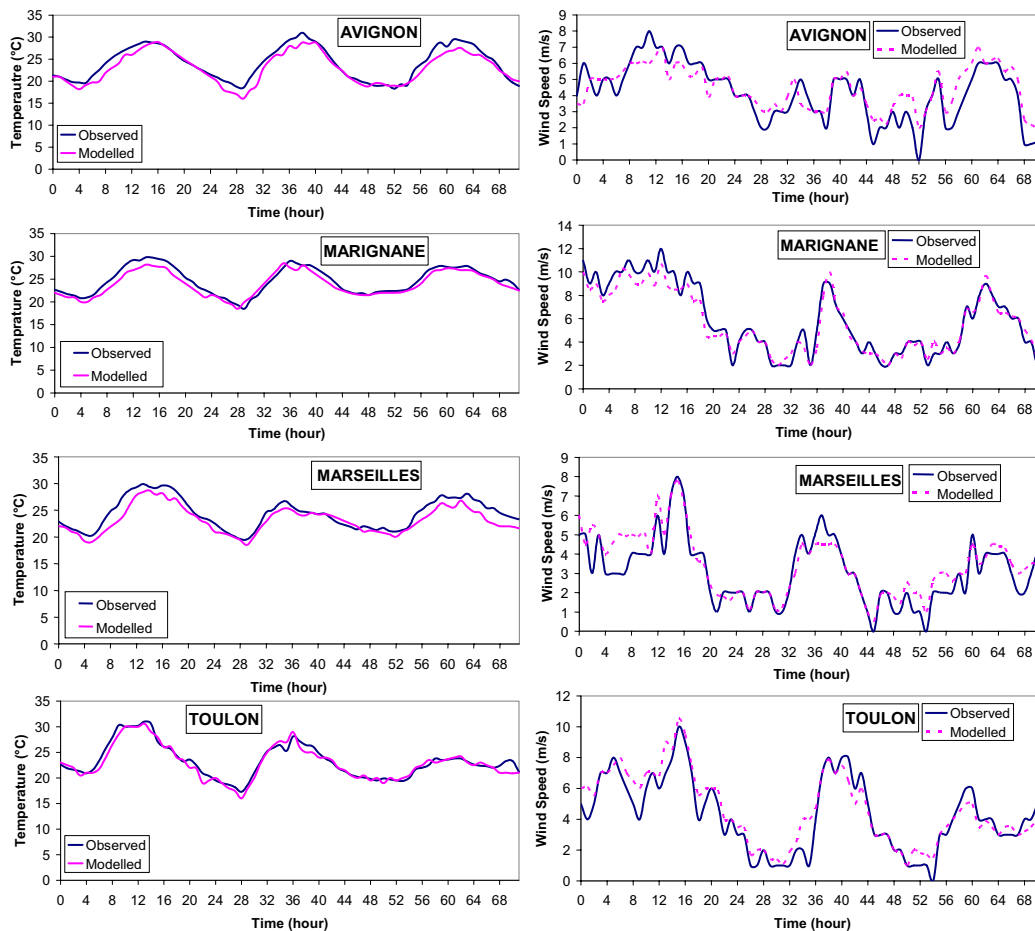
Fig. 4. Time variation (UTC) of temperature and wind speed from 29 June–1 July2000 for 4 cities, Avignon inland in north of ESCOMPTE domain, Marignane in center, Marseilles and Toulon in shore.

Title Page

Abstract | Introduction

Conclusions | References

Tables | Figures

◄◄ | ►►

◄ | ►

Back | Close

Full Screen / Esc

Print Version

Interactive Discussion
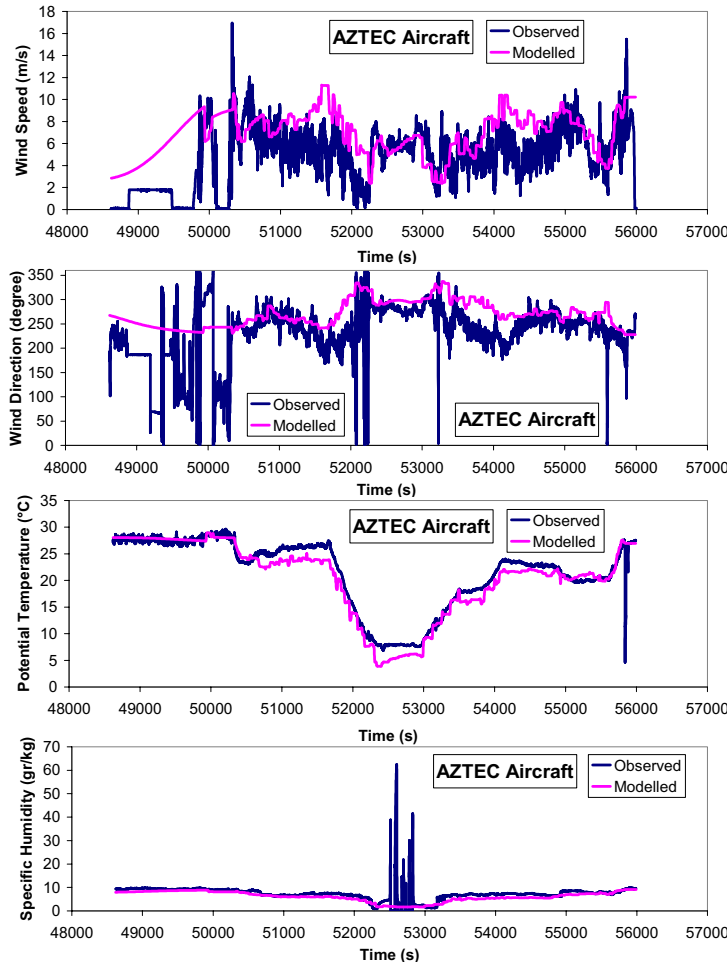
Fig. 5. Wind speed and direction, potential temperature and specific humidity for AZTEC plane (flight of 30 June 2000 at 13:59 UTC)
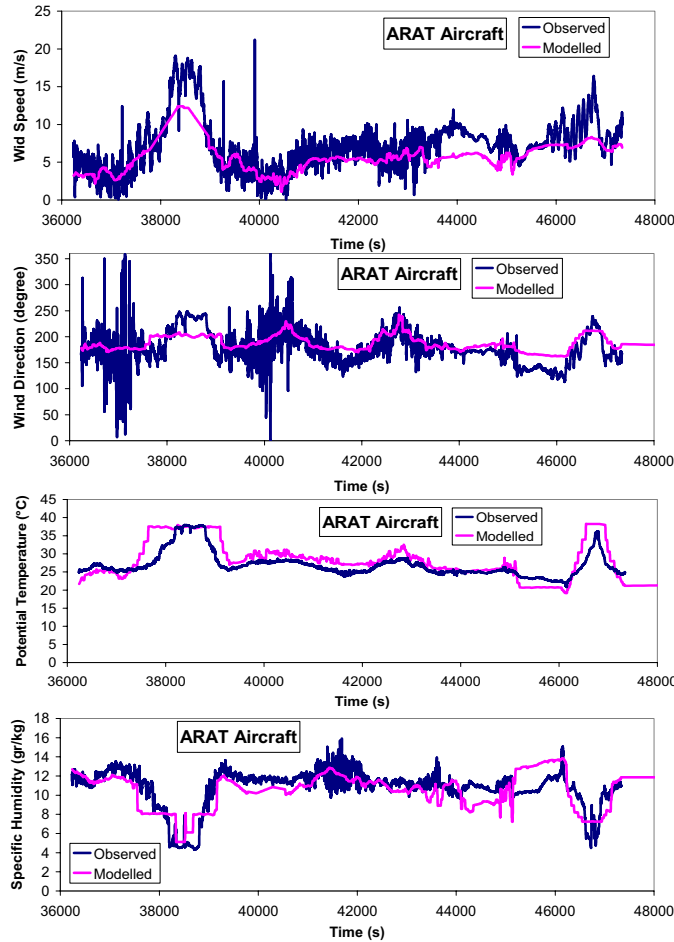
Fig. 6. Wind speed and direction, potential temperature and specific humidity for ARAT plane (flight of 1 July 2000 at 10:03 UTC).
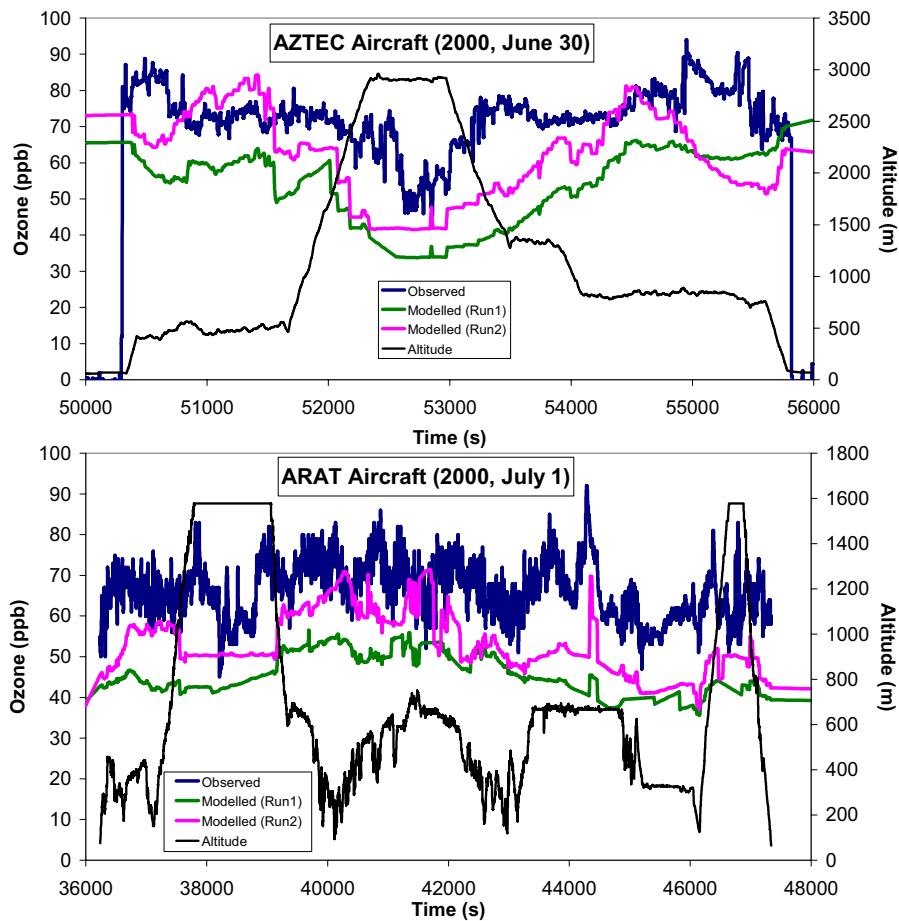
Fig. 7. Ozone concentration, observed with AZTEC plane (30 June 2000) and ARAT plane (1 July 2000), and modelled using only one grid (Run1) and using two nested grids (Run2).
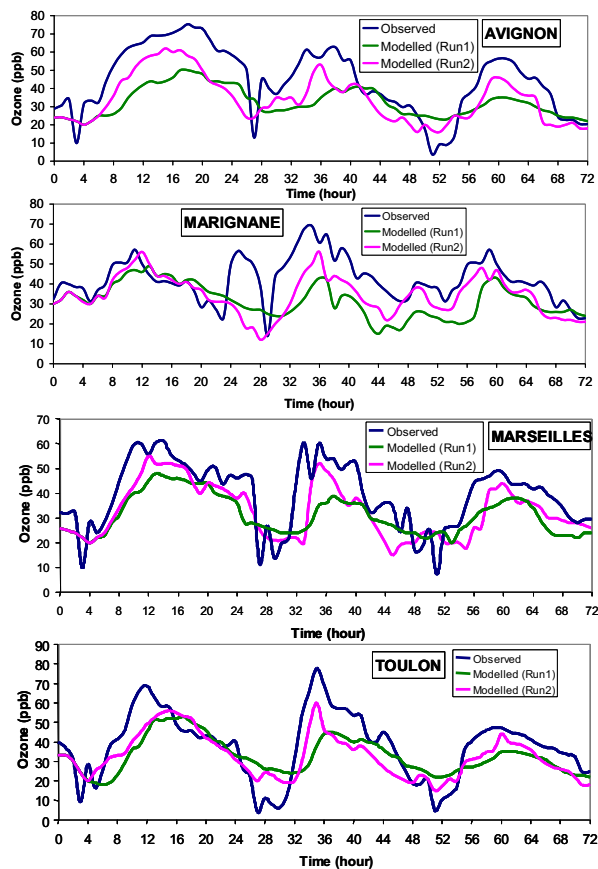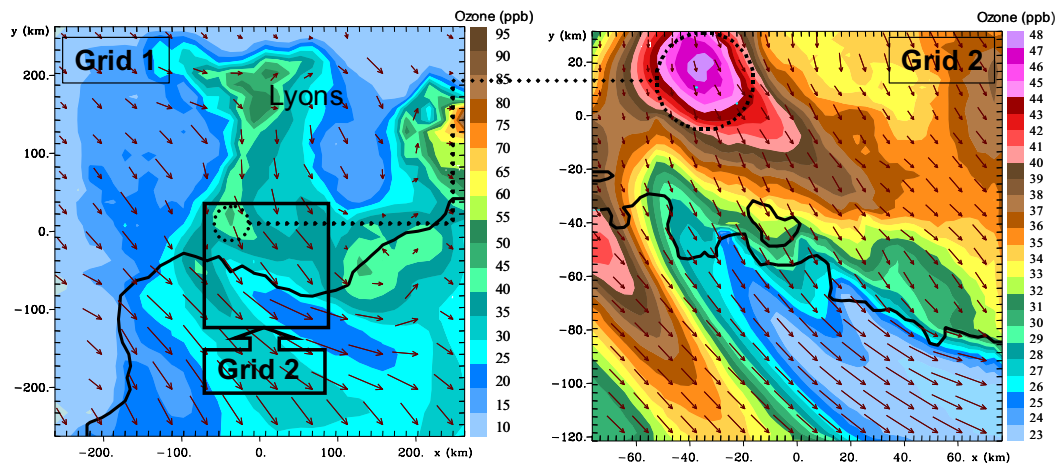
Fig. 8. Time variation (UTC) of observed and modelled (Run1 and Run2) ozone concentration (ppb) from 29 June–1 July 2000 for 4 cities: Avignon inland in north of ESCOMPTE domain, Marignane in center, Marseilles and Toulon in shore.

Fig. 9. Time variation (UTC) of observed and modelled (Run1 and Run2) NO_x, SO_2 and CO concentration (ppb) from 29 June–1 July 2000 for 3 cities: Avignon inland in north of ES-COMPTE domain, Aix-en-Provence close to center and Marseilles in shore.

Fig. 10. Ozone concentration (ppb) and Wind speed (ms^{-1}) – Left: Grid 1, Right: Grid 2; 29 June 2000 at 9:00 UTC